Chapter 1

Theory

In order to properly understand the RPND, the experimental measurements, and the models, it is necessary to develop a theoretical underpinning. The RPND is a form of plasma, which is in turn a type of ionized gas. Therefore, we begin with a review of the statistical description of an ionized gas, equilibrium solutions, and several approximations. Subsequently, the discharge initiation process is considered from the perspective of a single avalanche. The Townsend model is briefly reviewed, followed by a more detailed explanation of the streamer model. This naturally leads to the development of a homogeneous discharge condition based on the preionization density; the basis for the RPND. Following this, a qualitative introduction to atomic structure is provided in order to introduce spectroscopic concepts such as energy levels, transitions, lineshapes, and absorption cross sections.

1.1 Ionized Gas

An ionized gas is a volume of gas in which some fraction of the neutral atoms and/or molecules have been separated into electron and ion pairs. For a sufficiently large number of particles, the behavior of each species in the ionized gas can be described by a continuous distribution function.

This function is an expression of the likelihood of finding a particle with a specific range of velocities in a specific volume, as a function of time. This function is denoted as $f_\alpha(\vec{r}, \vec{v}, t)$, where the subscript α denotes the species, f is the distribution function, $\vec{r}$ is the position, $\vec{v}$ is the velocity, and t is the time.

The behavior of f_α can be shown [1] to be governed by the Boltzmann equation,

$$\frac{\partial f_\alpha}{\partial t} + \vec{v} \cdot \nabla f_\alpha + q_\alpha \left(\vec{E} + \vec{v} \times \vec{B} \right) \cdot \nabla_v f_\alpha = \left(\frac{\partial f_\alpha}{\partial t} \right)_{\text{coll}}. \tag{1.1}$$

Here, q is the charge of the species, $\vec{E}$ is the electric field, $\vec{B}$ is the magnetic field, and $(\partial f_\alpha / \partial t)_{\text{coll}}$ is a term which represents changes to the distribution function as a result of collisions. Coupled with Maxwell's equations, equation 1.1 provides a complete description of the behavior of the fields and particles in a plasma.

For a species in equilibrium in the absence of external forces and $(\partial f_\alpha / \partial t)_{\text{coll}} = 0$, it can be shown that the distribution of energies is

$$f_\alpha(\varepsilon) = \frac{3\sqrt{3}}{\sqrt{2\pi}} (k_{\text{B}} T_\alpha)^{-3/2} \exp\left(-\frac{3\varepsilon}{2 k_{\text{B}} T_\alpha} \right) \tag{1.2}$$

where ε is the energy, k_{B} is Boltzmann's constant, and T_α is the temperature of the species. This is referred to as the Maxwell-Boltzmann distribution. It should be emphasized that this solution only applies when the species can be considered

to be in equilibrium. Gradients and electromagnetic fields can both significantly alter the distribution function of a species. This can be of particular importance in the calculation or reaction rates, or the measurement of temperatures.

Additionally, the Boltzmann equation may be solved for electrons in equilibrium with a small, constant electric field, assuming they only interact through elastic collisions. This result was originally presented by Druyvesteyn and Penning [2] and has come to be known as the Druyvesteyn distribution. It is defined as,

$$f_\alpha = \frac{3\sqrt{3}}{4\Gamma(3/4)}(k_\mathrm{B}T_\alpha)^{-3/2}\exp\left[-\frac{9}{16}\left(\frac{\varepsilon}{k_\mathrm{B}T_\alpha}\right)\right] \tag{1.3}$$

where Γ is the gamma function. This solution tends to suppress the probability of higher and lower-energy electrons in favor of more intermediate values. Figure 1.1 compares the probability distributions from equations 1.2 and 1.3 for the same temperature α. The dotted line illustrates the average energy for the two distributions, which is not the same as the most probably energy.

Additional solutions of equation 1.1 in anything but these simple cases can be very challenging. Even computational approaches can be stymied by the seven-dimension phase space and high dynamic range. In most situations, the Boltzmann equation is reduced to more tenable expressions by integrating over velocity-space (leaving f as a function of space and time). The first so-called moment is the conservation equation or continuity equation,

$$\frac{\partial n_\alpha}{\partial t} + \nabla\cdot(n_\alpha\vec{u_\alpha}) = G_\alpha - L_\alpha. \tag{1.4}$$

In this case, there is now a mean velocity $\vec{u}$, as well as gain (G) and loss (L)

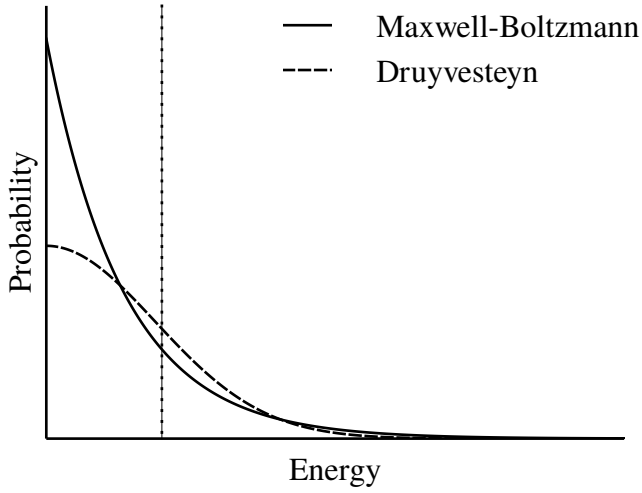

Figure 1.1: Comparison of the Maxwell-Boltzmann energy distribution and the Druyvesteyn distribution for the same average energy (illustrated by the dotted line).

terms which replace the collision operator. The gain and loss terms are generally expressed as the product of the densities of the interacting species, and a rate coefficient. For an electron-impact interaction where the target is relatively stationary, the rate coefficient is

$$K = \int_0^\infty f_e(\varepsilon)\sigma(\varepsilon)\sqrt{\frac{2\varepsilon}{m_e}}d\varepsilon, \tag{1.5}$$

where σ is the energy-dependent cross section.

The definition of the mean velocity, $\vec{u}$ can be obtained by multiplying equation 1.1 by v and integrating over velocity-space, to obtain the second moment,

$$m_\alpha n_\alpha \left[\frac{\partial \vec{u_\alpha}}{\partial t} + (\vec{u_\alpha}\cdot\nabla)\vec{u_\alpha}\right] = q_\alpha n_\alpha(\vec{E} + \vec{u_\alpha}\times\vec{B}) - \nabla\cdot\vec{\Pi} + \vec{f}|_{\text{coll}}. \tag{1.6}$$

This expresses the conservation of momentum by the plasma. It provides a means by which to solve for the mean velocity of the system, however it also introduces two additional terms. $\vec{f}|_{\text{coll}}$ deals with the forces transferred to α via collisions. This is often approximated as the Krook collision operator, which is only dependent on known quantities. The second term, $\vec{\Pi}$, is the pressure tensor and can only be defined by the third moment of the Boltzmann equation. In fact, each additional moment introduces a new term requiring a higher order moment, *ad infinitum*. In most situations, this chain of equations is terminated after the first two or three moments by the use of an additional assumption such as an equation of state.

For the purposes of this paper, one more moment will suffice. Assuming that the pressure is isotropic, one can multiply equation 1.1 by $mv^2/2$, and integrate over velocity-space to find the energy conservation equation,

$$\frac{\partial}{\partial t}\left(\frac{3}{2}p_\alpha\right) + \nabla\cdot\frac{3}{2}(p_\alpha\vec{u}_\alpha) + p_\alpha\nabla\cdot\vec{u}_\alpha + \nabla\cdot\vec{q}_\alpha = \frac{\partial}{\partial t}\left(\frac{3}{2}p_\alpha\right)\Bigg|_{\text{coll}}. \tag{1.7}$$

In this case, p represents the isotropic pressure, and $\vec{q}$ is the heat flow. The first term on the LHS represents the total energy contained by the species, the second term is the energy flux in and out of the volume, and the third term accounts for changes due to compression or expansion. The RHS is the collision operator which describes energy added or removed from the system as a result of collisions.

Equations 1.4 and 1.7 are particularly important for this study. As will be detailed in chapter **??**, the two can be used to create a global model of the plasma. Such a model assumes spatial homogeneity of the plasma in order to reduce the

associated computational costs. This allows the model to address large numbers of species over long periods of time as will be required in the case of the RPND.

1.2 Plasma Criteria

Though the Boltzmann equation describes both an ionized gas and a plasma, the two are distinct as a plasma is necessarily an ionized gas, but not vice versa. A plasma is unique in that its dynamics are governed by long range electromagnetic forces, unlike gases in which short-range collisions dominate. As a result, plasmas frequently exhibit large scale structure and organization. Examples of these structures are ubiquitous in astronomy where phenomena such as the aurora borealis, coronal mass ejections, and even interstellar media are all plasmas. There are three criteria which form a more exact definition of what constitutes a plasma.

Debye Length

If an electrical perturbation is introduced into an ionized gas, the charged particles will tend to rearrange themselves to shield it out. A plasma is an ionized gas which is large enough for this shielding effect to occur. The characteristic length scale for this shielding effect to take place is referred to as the Debye length, denoted λ_D. It can be shown to be equal to $\sqrt{\varepsilon_0 T_e/(en_0)}$, where ε_0 is the vacuum permittivity, T_e is the electron temperature, and n_0 is the plasma density. If the characteristic length scale of the ionized gas is L, then $\lambda_D < L$ for it to be

considered a plasma.

Debye Sphere

However, the above condition by itself is not sufficient for shielding to occur. It is possible that an ionized gas may have a relatively small Debye length, but also lack enough charged particles for shield to occur. More simply put, it would be impossible for a single electron to shield out even the smallest of perturbations. For that reason, the number of particles in a Debye sphere must be greater than unity in a plasma, or $n_0(4\pi\lambda_D^3/3) >> 1$.

Plasma Oscillations

Finally, a plasma may exhibit Debye shielding, but lack the collective behavior of a plasma. This can occur when the collision frequency with neutral particles is too high. In this case, the behavior of the ionized gas would be determined more by the random collisions. Therefore, the characteristic response frequency of a plasma, commonly called the plasma frequency, must be greater than the neutral collision frequency, or $\omega_p > \nu$. The plasma frequency can be shown to be $\omega_p = \sqrt{e^2 n_0/(\varepsilon_0 m_e)}$.

There are many natural and man-made plasmas of varying size and quality. Figure 1.2 shows several categories of plasma, plotted as a function of their electron density and temperature. As can be seen, the electron densities span seven decades, and the densities cover in excess of 20. This broad range of conditions

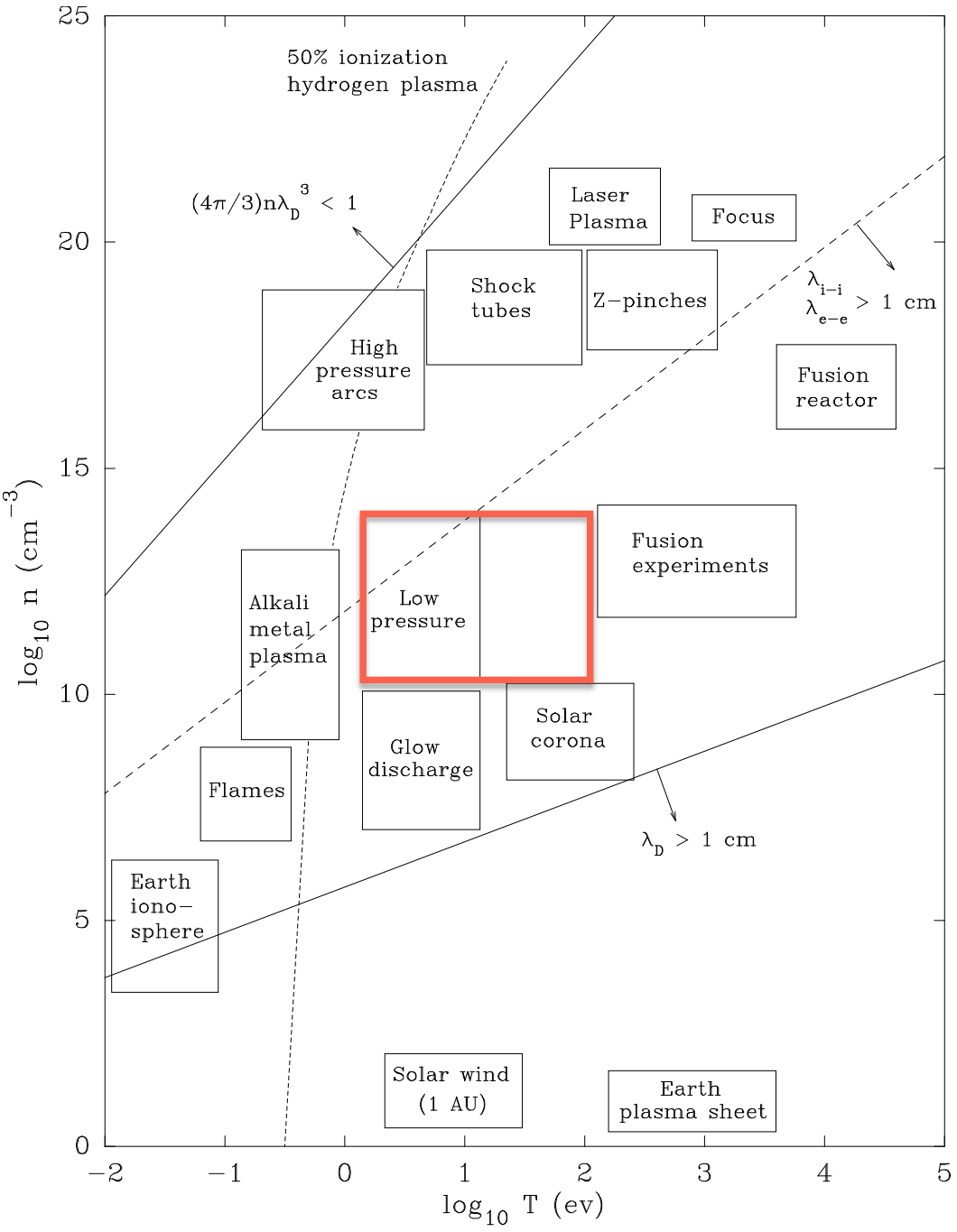

Figure 1.2: Illustration of the various regimes of plasma in terms of electron temperature and density with the RPND regime highlighted [3].

presents a particularly challenging problem for both simulations and experimental measurements. Also highlighted in the figure is the range spanned by the RPND.

1.3 Discharge Initiation

The Boltzmann equation is a continuous, statistical description of a plasma. By comparison, the initial breakdown of a plasma is a highly discontinuous process marked by its stochasticity. The initiation of a discharge is typically the result of electron avalanches which occur randomly throughout a volume of gas. Often, the seed electrons for a plasma are the products of ionizing cosmic rays. At sea level this results in a few electrons per cubic-centimeter. As a result, it is necessary to consider the initiation of a discharge separately from a pre-existing plasma.

Townsend Mechanism

Classically, plasmas are created by two different mechanisms, the applicability of which depends on primarily on the strength of the electric field relative to the neutral gas density, a value called the reduced electric field. At lower reduced fields, the Townsend mechanism is responsible for the formation of a plasma. Consider two electrodes separated by a gap filled with some gas. An electron starting near the cathode will drift toward the anode. For a large enough electric field the electron will gain sufficient kinetic energy to ionize a neutral atom,

producing a second electron. The two electrons are now accelerated by the field, instigating further ionization of the background gas. The population of electrons quickly grows, thus the process is referred to as an electron avalanche. Eventually, the avalanche electrons are collected at the anode.

In their wake are ions which slowly drift toward the cathode. As the ions impact the surface of the cathode, they occasionally cause a secondary electron to be emitted. This secondary electron initiates a new avalanche and helps to sustain the discharge. A steady state electric discharge occurs when the electron multiplication in the avalanche compensates for the finite probability that an ion striking the cathode releases a secondary electron. Therefore, the characteristic time for a Townsend discharge to develop is approximately equal to the time it takes an ion to drift across the gap (for a gap of several cm this can be on the order of 10^{-4} s).

The Townsend mechanism is characterized by two parameters: α and γ, the first and second Townsend coefficients. α is the number of ionization events that occur per unit length, often expressed as a function of the reduced field. The second Townsend coefficient is the probability that an ion impinging on the cathode produces a secondary electron. The values for γ can vary widely and depend on the type of ion, its energy, the cathode material, contamination of the surface, and many other factors. That said, typical values are around 0.01-0.1.

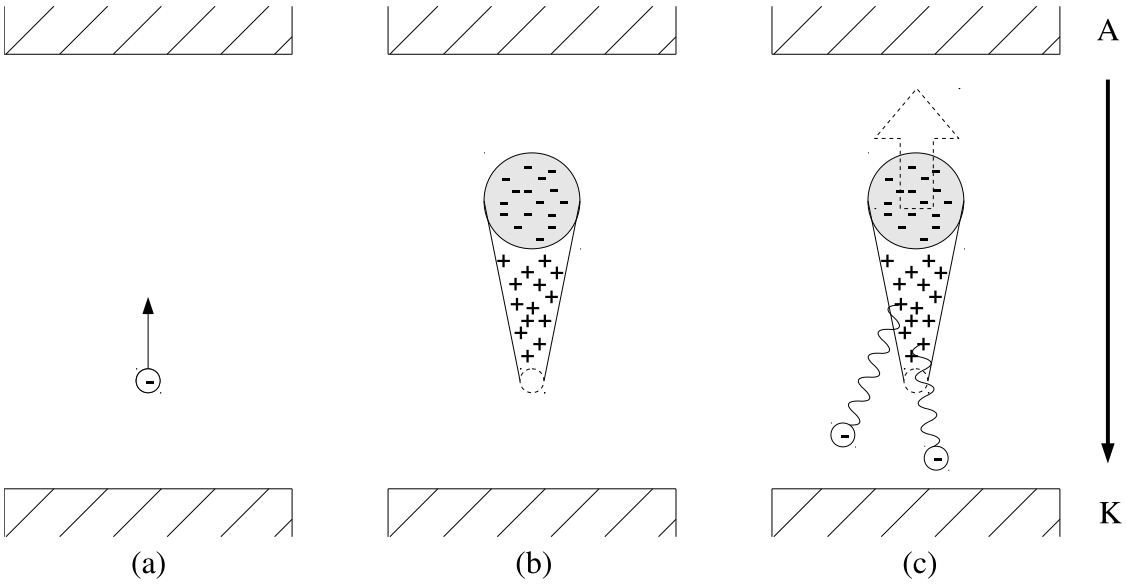

Figure 1.3: An illustration of the development of a single streamer. (a) A seed electron is accelerated by the applied electric field. (b) The initial electron develops into an avalanche which leaves a large region of positive space charge, halting further advance. (c) The streamer propagates toward the cathode via photoionization and the anode via nonlocal electrons and photoionization.

Streamer Mechanism

In contrast, the streamer discharge which occurs for larger values of the reduced field does not depend on secondary emission. Additionally, streamer discharges can develop in time periods as short as 1 ns, much less than the time required for Townsend breakdown. In order to describe the streamer mechanism, again consider an electron between two electrodes, as seen in (a) of figure 1.3. As with the Townsend discharge, this electron initiates an avalanche which moves toward the anode. As the electrons travel toward the anode, they randomly collide and diffuse, leaving behind a cone of ions, as seen in part (b). However, the

higher reduced field drastically increases α. This causes the space charge of the avalanche to create an electric field comparable to the one that is applied, quickly halting the avalanche.

Once stalled, the avalanche can no longer continue to advance toward either electrode. At this point the avalanche can be considered a streamer as it begins to increase its extent by several other processes. The large internal fields of the avalanche can accelerate individual electrons and "inject" them in the direction of the anode [4]. In addition, as the excited atoms in the wake of the avalanche begin to radiate, they can cause photoionization throughout the volume. Photoelectrons generated close enough to the negative head, or positive tail of the streamer will initiate secondary avalanches which eventually connect to the primary one. Both of these methods take place primarily along the axis of the original avalanche, thus the streamer remains relatively constricted in the direction transverse to the electric field.

Homogeneity Condition

However, these processes are not critical in the formation of a large-volume discharge by an RPND. This description of a streamer only considers an avalanche generated by a single electron. In reality, many can form simultaneously assuming that there is more than one seed electron in the volume. With sufficient preionization of the volume, the strong fields of the individual avalanches can begin to overlap. This smoothes out the field gradients which would otherwise radially constrict the streamers. Instead, ionization progresses homogeneously

throughout the volume.

In order to determine the necessary preionization density, we refer to the work done by Levatter and Lin on gas laser discharges [5]. First, the electron drift velocity in an applied field can be expressed as the product of the field and the electron mobility μ. The electron mobility is the steady-state drift velocity for an electron in an applied field and represents the balance between the frictional force of the neutral gas collisions and the electric field. Consequently, the mean velocity of electrons drifting in a time-varying field $E(t)$ can be expressed as

$$u(t) = \mu(E)E(t). \tag{1.8}$$

This allows the length of the avalanche can then be written as an integral quantity,

$$\xi = \int_{t_0}^{t} u(t)dt. \tag{1.9}$$

Here, t_0 is the time at which $E(t)$ becomes high enough that the first Townsend coefficient, α, exceeds 0. Because no electron multiplication occurs while $\alpha < 0$, this effectively represents the beginning of the avalanche.

The electric field in the head of the avalanche depends on its radius, which is dependent on the diffusion of the electrons as they cross the gap. This is governed by the free diffusion coefficient, $D = \lambda v_m athrmth(E)/3$, where λ is the mean free path of the electrons, and v_{th} is their thermal velocity. The diffusion radius is then equal to

$$R(\xi) = \int_{0}^{\xi} \lambda v_{\mathrm{th}}(\xi')d\xi'. \tag{1.10}$$

For the calculations below, λ is assumed to be fixed. In contrast, the thermal velocity of the electrons is expected to grow as the electric field deposits energy in the electrons. As a result, it is necessary to integrate the diffusion coefficient over the avalanche in order to determine R.

Levatter and Lin assume that the avalanche stalls when the peak field of the avalanche is equal to the applied field. Assuming that the electrons diffuse equally in all directions, the electric field of the avalanche head can be expressed as

$$E_a(r) = \frac{eN_e}{4\pi\varepsilon_0 R^2} F(r/R), \qquad \text{where} \tag{1.11}$$

$$F(r/R) = \frac{1}{R^2}\left[\mathrm{erf}(r/R) - \frac{2}{\pi^{1/2}}(r/R)\exp(-r^2/R^2)\right], \tag{1.12}$$

where r is the radius with respect to the center of the avalanche, N_e is the number of electrons in the avalanche, erf is the error function. F is a dimenionless function which has a peak value of 0.428. Provided α as a function of reduced field, the number of electrons in the avalanche is equal to

$$N_e = \int_0^{\xi} \alpha(\xi')d\xi'. \tag{1.13}$$

Here, Levatter and Lin make a number of assumptions in order to develop an analytic and dimensionless solution for $E_{a,\max}(t) = E(t)$. However, it is possible to numerically integrate equations 1.9, 1.10, and 1.13 to determine the time required for the avalanche to stall. This should provide a more accurate, but less general result. Assuming a linearly increasing electric field, figure 1.4 shows the results of such calculations for an avalanche in 1.0 Torr of helium, as a function of various breakdown delays. The breakdown delay is defined as the time it takes for

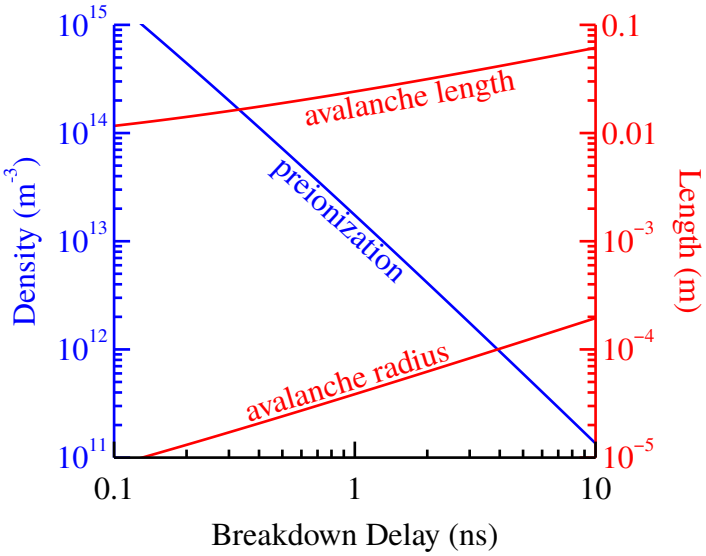

Figure 1.4: Numerical calculations of the preionization density for homogeneous excitation, avalanche length, and avalanche radius in helium at a pressure of 1.0 Torr as a function of the slope of the electric field.

$\alpha > 0$. The mobilities, mean velocities, and Townsend coefficients were interpolated from solutions of the Boltzmann equation provided by the BOLSIG+ code with Phelps' cross sections [6]. For this range of breakdown delays, the avalanche was able to develop up to 6 cm in length before it stalled. The times required for the avalanche to stall ranged from around 13 ns for the shortest breakdown delay, and 330 ns for the longest.

From this, a criteria for homogeneous breakdown of the gas can be developed. In order for the field gradients to be smoothed out, the individual avalanche heads should roughly overlap by the time they have stalled. Assuming that all seed electrons in the volume initiate avalanches, this is equivalent to the requirement

that $n_{e,c} > r_c^{-3}$, where $n_{e,c}$ is the critical electron density, and r_c is the avalanche radius at stall. As seen in figure 1.4, this suggests that a preionization density of 10^{11} to 10^{15} is required for the breakdown times under consideration.

Based on this formulation for the homogeneous breakdown condition, tt is apparent that as the avalanche radius increases, the necessary preionization density decreases. It is less obvious as to why the avalanche radius decreases as the breakdown delay increases. This can be explained by the lower slope, implied by the long breakdown delays. As the slope decreases, the avalanche has a longer period of time to diffuse in the system, thus the increased radius.

1.4 Atomic Spectroscopy & Notation

As described, much of the experimental work presented will concern the use of spectroscopic techniques. Careful measurements of the light emitted from excited atomic states can yield electron densities and temperatures, excited state densities and temperatures, electric fields, and magnetic fields. The topic of spectroscopy is extensive and it is neither necessary nor desirable to cover it in full. Instead we will only consider what is necessary to understand the emissions from a singly-excited, multi-electron atom.

An atom is composed of a small, positively charged nucleus, orbited by negatively charged electrons. The actual position of any single electron is probabilistic and described by a wavefunction or state; solutions of the Schrödinger equation for the atom in question. Many different wavefunctions exist, each described by

four quantum numbers:

- $n = 1, 2, \ldots$: the principal quantum number,
- $l = 0, 1, \ldots, n-1$: the azimuthal angular momentum,
- $m_l = -l, \ldots, l$: the magnetic quantum number, and
- $s = \pm 1/2$: the spin quantum number.

The quantum numbers are hierarchical such that each n, or shell, possesses a series of subshells, l, while each subshell possesses a number of individual orbital, m_l, and each orbital possess one of two spins. As a result of the Pauli exclusion principle, the wavefunction of each electron around an atom is described by a *unique* set of quantum numbers. This means, that any particular subshell can only contain $2(2l+1)$ electrons. The subshells are often referred to using the nomenclature $0, 1, 2, 3, \ldots = s, p, d, f, \ldots$.

As a result of their separation from the nucleus, the electrons in an atom have some degree of potential energy. As the n and l of an electron increase, so does its potential energy. In most cases, m_l and s do not affect the potential energy of an electron. As an example, an electron in the 1s ($n = 1$ and $l = 0$) subshell has the lowest possible potential energy.

Absent from external influences, the individual states are populated with electrons so as to minimize the total potential energy of the system. This natural arrangement is referred to as the ground state configuration. Often, but not always, the subshells are filled sequentially and in order from lowest to highest l. Pro-

vided some input energy in the form of a collision or a photon, one or more of the electrons surrounding the atom may transition to another state, increasing the potential energy of the system. In low-temperature plasmas it usually one of the electrons from the outermost or unfilled subshell to be excited.

In hydrogen and alkali metals, several subshells are filled with the exception of a lone outer (or valence) subshell with a single electron. For these atoms, the potential energy of any singly-excited configuration is uniquely determined by this electron. As a result, the initial and final states of the atom can be uniquely identified based on the initial and final n and l of the aforementioned electron. In contrast, the potential energies of configurations in other atoms are determined by the collective effects of all outer electrons. This includes the total azimuthal angular momentum $L = \sum l_i$, the total spin, $S = \sum s_i$, and the total angular momentum, $J = L + S$, where i are all the electrons of the valence shell. In addition, each state can be said to have either even or odd parity, defined as $(-1)^{\sum l_i}$, where -1 is odd, and 1 is even.

Together, these values are sufficient to identify the potential energy of the electron configuration. They are written with the internal shell configuration, followed by the "term symbol" for the outer subshell. One example of this term symbol is $1s2s\,^3S_1^o$, which describes the triplet helium metastable state. In this case, there is a single electron in the 1s subshell and a second atom in the 2s subshell. The configuration has a total azimuthal angular moment of 0 (denoted by the 'S'), an odd parity (denoted by the superscript 'o'), a total spin of $1/2$ (the superscript 3 is equal to $2S + 1$) and a total angular moment of 1.

The total angular momentum can often take on a range of values, called levels, depending on the individual l and s states. This is caused by a process known as spin-orbit coupling. The energy difference between configurations with different total angular momenta is very small, generally less than 1 eV. In addition, within each level is a number of degenerate configurations; configurations with different arrangements of electrons, but the same energies.

Excited atomic states usually have finite lifetimes. If possible, electrons will undergo transitions to lower the potential energy of the system. This can occur spontaneously, through the emission of a photon, or through a superelastic collision with another particle. In the case of spontaneous transitions, only certain states can transition to others, as defined by a series of selection rules:

- $\Delta S = 0$
- $\Delta L = \pm 1$ or 0
- $\Delta J = \pm 1$ or 0
- $L = 0$ cannot transition to $L = 0$
- $j = 0$ cannot transition to $J = 0$

These rules are determined from a lower order approximation, and thus are not strict. As a result, forbidden transitions can occur, however these generally take place at much lower rates.

Figure 1.5 is a Grotrian diagram of the energy levels in neutral helium and the allowed transitions. In this case, the atomic states are separated into the singlet

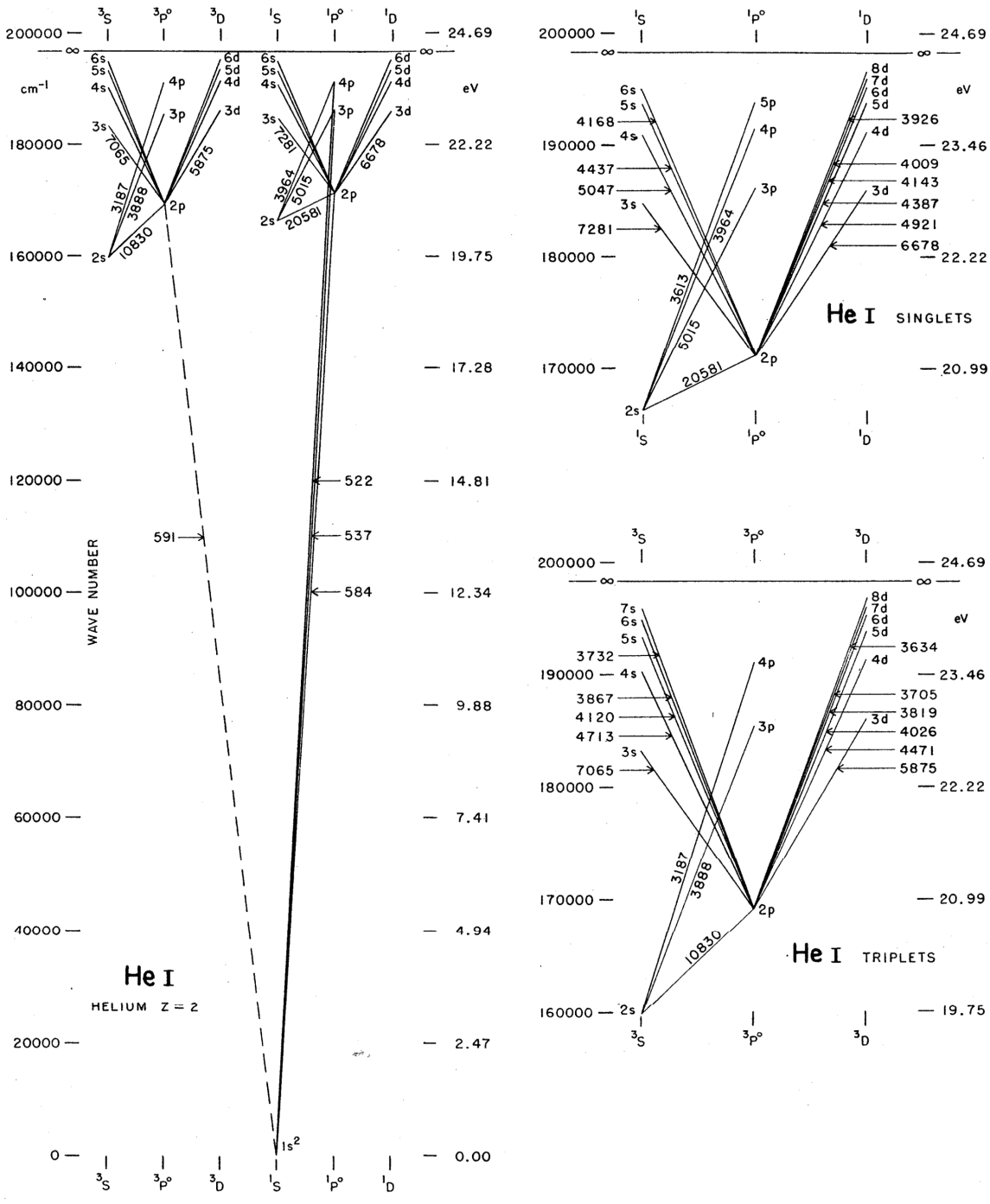

Figure 1.5: A partial Grotrian diagram of neutral helium [7].

($S = 0$) and triplet ($S = 1$) manifolds. The singlet manifold represents excited states where the electron spins are anti-parallel, and the triplet manifold represents excited states where the electron spins are parallel. As indicated by the first selection rule, transitions between these two manifolds is forbidden, thus each is something of a self-contained system.

Also observable in the diagram are two "metastable" states. These are the 2s states at the bottom of the singlet and triplet diagrams. An electron in either state cannot spontaneously transition to a lower energy state. As a result, an electron in either state can be extremely long-lived. In addition, they are also the lowest-lying excited states of helium. For these reasons, helium plasmas tend to have high densities of metastable atoms. This makes them a good candidate for spectroscopic study as will be seen in chapter **??**.

Spectral Lineshapes

Electrons which transition to lower energy states emit photons which can be detected. Conversely, if an atom is exposed to a photon with an energy matching a transition, the atom may absorb the photon. Both processes are useful in determining the prevalence and dynamics of the excited states. This, in turn, can be used to infer various plasma properties.

Conservation of energy requires that the energy of the absorbed or emitted photon match the energy difference between the two states. However, the finite lifetime of excited atomic states implies, via the time-energy formulation of the uncertainty principle, some uncertainty in the actual energy difference between

the states. As a result, the emitted photon will possess an energy selected from a distribution of energies.

This distribution is referred to as the spectral lineshape. The narrowest permissible lineshape, or natural lineshape, of an atomic transition can be shown [8] to be a Lorentzian of the form,

$$g(\omega) = -\frac{1}{4\pi^2}\frac{A\lambda^3}{\Delta\omega_a}\frac{1}{1+\left[2(\omega-\omega_a)/\Delta\omega_a\right]^2}, \tag{1.14}$$

where ω is the photon frequency, A is the Einstein coefficient for the transition, λ is the wavelength of the transition, ω_a is central frequency of the transition, and $\Delta\omega_a$ the full-width half maximum (FWHM) of the transition. In the ideal case, where the atoms motionless and unaffected by external perturbations, $\Delta\omega_a = A$. This is known as the natural linewidth.

Other processes can act to broaden or alter the spectral lineshape. For example, inter-atomic collisions can reduce the lifetimes of excited states. This results in additional broadening of the line, though it retains its Loretnzian nature. As the frequency of inter-atomic collisions increases linearly with pressure, this phenomena is referred to as pressure broadening. It can be included in equation 1.14 by using $\Delta\omega_a = A + BP$, where B is a measured or calculated broadening coefficient, and P is the pressure.

Atomic motion can also play a role in the spectral lineshape. If an atom is moving toward or away an observer as it emits a photon, the emitted photon will be blue or red shifted. Likewise, if the atom is moving toward or away an incident photon, the energy of that photon will be shifted. If this effect is averaged over

the random motion of atoms in a gas, the result is an additional broadening of the lineshape, called Doppler broadening. Unlike pressure broadening, Doppler broadening introduces a Gaussian component to the lineshape such that,

$$g(\omega) = \sqrt{\frac{2\ln 2}{\pi^3}}\frac{\Delta\omega_a}{\Delta\omega_d}\int_{-\infty}^{\infty}\frac{1}{[(\omega-\omega_a)-\omega']^2+4\Delta\omega_a^2} \times \exp\left[4\ln 2\left(\frac{\omega'}{\Delta\omega_d}\right)^2\right]d\omega'. \quad (1.15)$$

Here, $\Delta\omega_d = \omega_a\sqrt{\frac{8k_B T_g \ln 2}{Mc^2}}$, is the width of the Doppler broadening. This form of the spectral lineshape is known as the Voigt profile, and it must be numerically integrated. In the case that $\Delta\omega_d >> \Delta\omega_a$, equation 1.15 can be simplified to a standard Gaussian distribution,

$$g(\omega) = \sqrt{\frac{4\log 2}{\pi\Delta\omega_d^2}}\exp\left[-(4\log 2)\left(\frac{\omega-\omega_a}{\Delta\omega_d}\right)^2\right]. \quad (1.16)$$

The effect of the various broadening mechanisms is most apparent in the wings of the lineshape, far from the peak. Figure 1.6 illustrates the three major lineshapes with equivalent full widths. The Voigt profile is composed of equally broad Lorentzian and Gaussian distributions. As can be seen, the wings of the Gaussian distribution fall off very quickly. In comparison, the Lorentzian component is observable well out to the edges of the figure.

The spectral lineshape can be altered by a number of other processes. Electric fields can influence the emissions via the Stark effect, while magnetic fields can split up degenerate states via the Zeeman effect. The fields of electrons and nearby molecules can also alter the lineshape of a transition. While not used in this study, such effects can be used as effective diagnostic tools for plasmas.

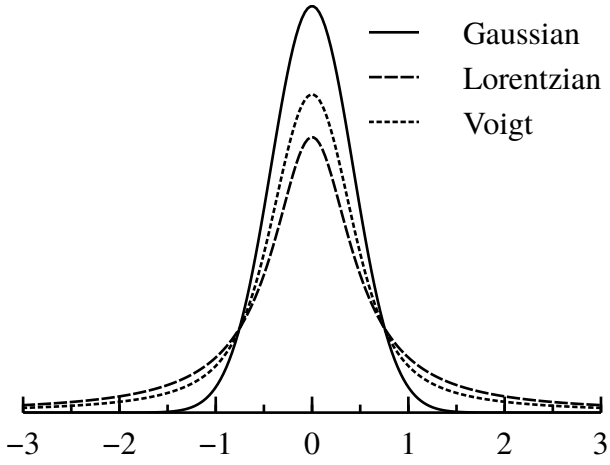

Figure 1.6: A comparison of the three primary spectral lineshapes, each with the same full width.

Absorption

As has been mentioned, a photon which closely matches the energy between two states can be absorbed by an atom. This property forms the basis for absorption spectroscopy where light with a known spectrum is used to illuminate a sample. The spectrum of the light that passes through the sample is measured and used to infer properties of the sample. In contrast to the emission processes occur spontaneously with a characteristic lifetime, often 10s of nanoseconds or more, absorption is almost instantaneous. This makes absorption-based spectroscopic methods desirable for fast phenomena, such as the RPND.

The cross section for a single atom to interact with a photon can be shown [8]

to be,

$$\sigma(\omega) = A\frac{\lambda^2}{8\pi}\frac{g_1}{g_2}g(\omega). \tag{1.17}$$

where g_1 and g_2 are the number of degenerate configuration for the lower state and upper state respectively. $g(\omega)$ is the appropriate spectral lineshape, determined from the operating conditions.

It is important to recognize that for absorption spectroscopy can also perturb the system it is measuring. In the above example, suppose two consecutive photons were incident on the atom. If the first was absorbed, the cross section for the second would be zero. This known as saturation and depends on the intensity of the photon field and the A coefficient for the transition. Assuming that saturation is the intensity required to reduce the absorption cross section by half, then the intensity limit for a two-state system is,

$$I_s = \frac{2\sqrt{2}h\nu_0 A}{\lambda^2}, \tag{1.18}$$

where h is Planck's constant, and ν_0 is the nominal frequency of the transition.

Bibliography

[1] Paul M. Bellan. *Fundamentals of Plasma Physics*. Cambridge University Press, 2008.

[2] M. J. Druyvesteyn and F. M. Penning. The Mechanism of Electrical Discharges in Gases of Low Pressure. *Reviews of Modern Physics*, 12(2):87–174, April 1940.

[3] J D Huba. *NRL Plasma Formulary*. Naval Research Laboratory, Washington, D.C., 2011.

[4] E Kunhardt and W Byszewski. Development of overvoltage breakdown at high gas pressure. *Physical Review A*, 21(6):2069–2077, June 1980.

[5] Jeffrey I. Levatter and Shao-Chi Lin. Necessary conditions for the homogeneous formation of pulsed avalanche discharges at high gas pressures. *Journal of Applied Physics*, 51(1):210, 1980.

[6] A V Phelps. Compilation of Electron Cross Sections, 2002.

[7] Charlotte E Moore and Paul W Merrill. Partial Grotrian Diagrams of Astrophysical Interest. Technical report, National Bureau of Standards, Washington, D.C., 1968.

[8] A. E. Siegman. *Lasers*. University Science Books, Sausalito, CA, 1986.